

# **Co-occurrence of Photochemical and Microbiological Transformation Processes in Open-Water Unit Process Wetlands**

Carsten Prasse<sup>1,2</sup>, Jannis Wenk<sup>1,3,#</sup>, Justin T. Jasper<sup>1</sup>,  
Thomas A. Ternes<sup>2</sup>, David L. Sedlak<sup>1,\*</sup>

<sup>1</sup> ReNUWIt Engineering Research Center and Department of Civil & Environmental Engineering,  
University of California at Berkeley, Berkeley, California 94720, United States

<sup>2</sup> Department of Aquatic Chemistry, Federal Institute of Hydrology (BfG), Koblenz, Germany

<sup>3</sup> Department of Chemical Engineering and Water Innovation & Research Centre (WIRC),  
University of Bath, Claverton Down, Bath BA2 7AY, United Kingdom

\* Corresponding author: [sedlak@berkeley.edu](mailto:sedlak@berkeley.edu)

Revised for Environmental Science & Technology

10/20/15

# Co-occurrence of Photochemical and Microbiological Transformation Processes in Open-Water Unit Process Wetlands

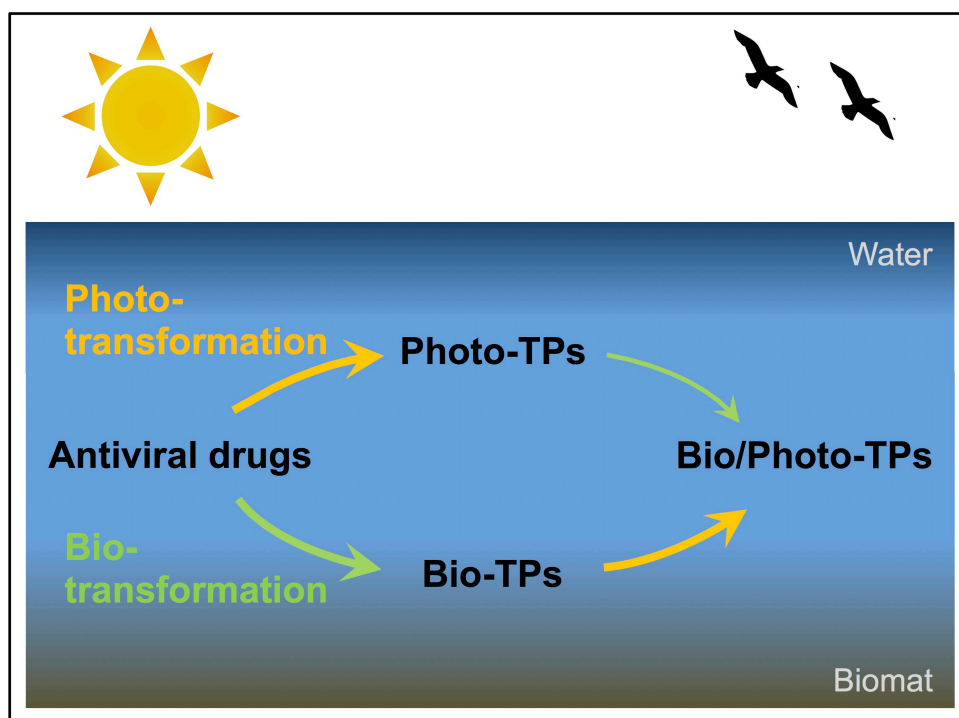
Carsten Prasse<sup>1,2</sup>, Jannis Wenk<sup>1,3</sup>, Justin T. Jasper<sup>1</sup>, Thomas A. Ternes<sup>2</sup>, David L. Sedlak<sup>1\*</sup>

<sup>1</sup> ReNUWIt Engineering Research Center and Department of Civil & Environmental Engineering, University of California at Berkeley, Berkeley, California 94720, United States

<sup>2</sup> Department of Aquatic Chemistry, Federal Institute of Hydrology (BfG), Koblenz, Germany

<sup>3</sup> Department of Chemical Engineering and Water Innovation & Research Centre (WIRC), University of Bath, Claverton Down, Bath BA2 7AY, United Kingdom

\*Corresponding author: sedlak@berkeley.edu



16  
17  
18  
19  
20

21 **Abstract**

22 The fate of anthropogenic trace organic contaminants in surface waters can be complex due  
23 to the occurrence of multiple parallel and consecutive transformation processes. In this  
24 study, the removal of five antiviral drugs (i.e., abacavir, acyclovir, emtricitabine, lamivudine  
25 and zidovudine) via both bio- and photo-transformation processes was investigated in  
26 laboratory microcosm experiments simulating an open-water unit process wetland  
27 receiving municipal wastewater effluent. Phototransformation was the main removal  
28 mechanism for abacavir, zidovudine and emtricitabine, with half-lives ( $t_{1/2,photo}$ ) in wetland  
29 water of 1.6 h, 7.6 h and 25 h, respectively. In contrast, removal of acyclovir and lamivudine  
30 was mainly attributable to slower microbial processes ( $t_{1/2,bio} = 74$  h and 120 h,  
31 respectively). Identification of transformation products revealed that bio- and photo-  
32 transformation reactions took place at different moieties. For abacavir and zidovudine,  
33 rapid transformation was attributable to the high reactivity of the cyclopropylamine and  
34 azido moiety, respectively. Despite substantial differences in kinetics of different antiviral  
35 drugs, biotransformation reactions mainly involved oxidation of hydroxyl groups to the  
36 corresponding carboxylic acids. Phototransformation rates of parent antiviral drugs and  
37 their biotransformation products were similar, indicating that prior exposure to  
38 microorganisms (e.g., in a wastewater treatment plant or a vegetated wetland) would not  
39 affect the rate of transformation of the part of the molecule that was susceptible to  
40 phototransformation. However, phototransformation strongly affected the rates of  
41 biotransformation of the hydroxyl groups, which, in some cases, resulted in greater  
42 persistence of phototransformation products.

43

44

45

46

47

48

49

50

51

## 52 **Introduction**

53 The discharge of municipal wastewater effluents into surface waters can result in the  
54 presence of trace organic contaminants at concentrations that pose potential risks to  
55 aquatic ecosystems and drinking water resources. After their release, many trace organic  
56 contaminants are attenuated by biological and photochemical processes. Although these  
57 processes often occur simultaneously or sequentially in the environment, most studies  
58 have considered the occurrence of only one transformation process at a time.<sup>1-4</sup> Thus, it is  
59 difficult to predict which transformation products will be formed and whether or not  
60 transformation reactions occurring at one moiety alter the kinetics of subsequent  
61 transformation reactions. Furthermore, if partial transformation of a compound enhances  
62 the reactivity of other moieties, interaction of transformation processes could result in  
63 changes in the distribution of transformation products as well as their rates of removal. For  
64 example, carbamazepine, a compound that is particularly resistant to biotransformation is  
65 slowly transformed upon exposure to sunlight via direct photolysis and reaction with  
66  $\cdot\text{OH}$ .<sup>5,6</sup> This leads to the formation hydroxylated derivatives,<sup>7</sup> which are more easily  
67 biodegraded than the parent compound.<sup>8</sup>

68 Open water unit process wetlands have been developed as a polishing treatment step for  
69 municipal wastewater effluents.<sup>9</sup> These managed natural systems utilize sunlight to  
70 remove trace organic compounds and inactivate pathogens.<sup>10-12</sup> In addition,  
71 microorganisms in the biomat formed at the bottom of these treatment basins reduce  
72 nitrate and contribute to aerobic biodegradation of trace organic contaminants.<sup>13,14</sup> To  
73 assess the importance of the co-occurrence of biological and photochemical transformation  
74 reactions to reaction kinetics and product distribution, the fate of five antiviral drugs (i.e.,  
75 abacavir, emtricitabine, lamivudine, zidovudine and acyclovir, see Figure 1) was studied  
76 under conditions comparable to those encountered in open-water unit process wetlands.  
77 Antiviral drugs were chosen because they are widely used for the treatment of diseases  
78 such as herpes, hepatitis and HIV, and have been detected at concentrations above  $1 \mu\text{g L}^{-1}$   
79 in municipal wastewater effluents.<sup>15-18</sup> No information about potential environmental  
80 effects resulting from the release of these compound into the aquatic environment is  
81 available so far. Furthermore, little is known about the effects of these compounds on

82 environmental viruses, a group of microorganisms that play a very important role in  
83 aquatic ecosystems.<sup>19</sup>

84 By investigating transformation kinetics and transformation mechanisms under conditions  
85 comparable to those encountered in open-water unit process wetlands it is possible to gain  
86 insight into how simultaneously occurring bio- and photo-transformation reactions affect  
87 the overall fate of antiviral drugs in sunlit surface waters. These compounds also serve as  
88 models for other families of compounds that contain moieties that are susceptible to bio-  
89 and phototransformation.

90

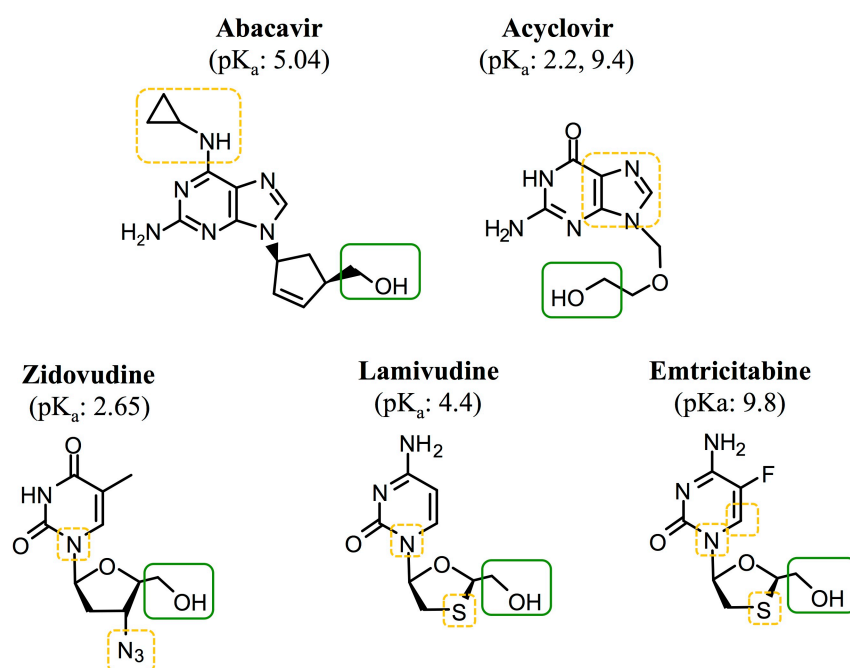


Figure 1. Antiviral drugs and their most likely sites of proposed photo- (□) and biotransformation (■) reactions.

91

## 92 **Materials and Methods**

### 93 *Chemicals*

94 Analytical reference standards of antiviral drugs and stable isotope-labeled analogues used  
95 as internal standards (purity > 99%) were purchased from Toronto Research Chemicals  
96 (Ontario, Canada). All other chemicals and solvents were obtained from Fisher Scientific  
97 (Fairlawn, NJ).

98

99 *Wetland water sampling conditions*

100 Phototransformation experiments were conducted in water collected from a pilot-scale  
101 open-water unit process wetland located in Discovery Bay, CA. The facility treats about  
102 10,000 gallons per day ( $4.4 \times 10^{-4} \text{ m}^3 \text{ s}^{-1}$ ) of nitrified wastewater effluent from an adjacent  
103 municipal wastewater treatment plant. Details about the open-water unit process wetland  
104 were described previously.<sup>10,13</sup> Water collected from the open-water wetland typically  
105 contained 10 - 20 mg L<sup>-1</sup> -N NO<sub>3</sub><sup>-</sup>, 5 - 10 mg L<sup>-1</sup>-C DOC, and 60 - 80 mg L<sup>-1</sup>-C dissolved  
106 inorganic carbon (HCO<sub>3</sub><sup>-</sup> and CO<sub>3</sub><sup>2-</sup>). Samples for laboratory irradiation experiments were  
107 collected from the mid-point of the wetland. All samples were filtered through pre-rinsed  
108 1µm (nominal pore size) glass fiber filters (Whatman) and were stored in the dark at 4°C  
109 until analysis, which occurred within 5 days.

110

111 *Laboratory photo- and biotransformation experiments*

112 Irradiation experiments were performed using a collimated beam Oriel Solar Simulator  
113 (Spectra Physics, serial no. 91194) equipped with a 1000 W Xe lamp and either two  
114 successive atmospheric attenuation filters (Spectra Physics, serial no. 81088 & 81017) or  
115 one atmospheric and one UVB-filter (Spectra Physics, serial no. 81088 & 81050). Spectral  
116 irradiance was routinely measured with a spectroradiometer (RPS 380, International light)  
117 at different locations of the irradiated area to assess variability, which was always < 5%.  
118 Details on lamp irradiance energies and the spectra of different configurations are given in  
119 section 1.1 of the Supporting Information (SI). Irradiation experiments were carried out in  
120 100 mL black-painted glass beakers that were placed in a water bath at constant  
121 temperature ( $18 \pm 2^\circ\text{C}$ ). Initial concentrations of antivirals of approximately 0.5 µM were  
122 used for all kinetics experiments. Pseudo-first order phototransformation rate constants of  
123 antivirals and photochemical probe compounds used for the quantification of  
124 concentrations of reactive intermediates were calculated from the slopes of linear  
125 regression of the natural log of concentration versus time. No degradation of antiviral  
126 drugs was observed in control experiments in the dark indicating that their transformation  
127 in filtered wetland water was only attributable to photochemical processes.

128 For the elucidation of biotransformation kinetics, beakers were additionally supplemented  
129 with 10 mL of the biomat taken from the bottom of a pilot-scale open-water wetland and  
130 kept in the dark (see Jasper et al.<sup>13</sup> for further details). Biodegradation of compounds  
131 followed pseudo-first order degradation kinetics, indicating stable conditions throughout  
132 the experiments. In addition, observed transformation rates in good agreement with  
133 results from a preliminary study used to design the more detailed experiments.

134

135 *Direct and indirect phototransformation.* Experiments to assess direct phototransformation  
136 of antiviral drugs were conducted in buffered ultrapure water at pH-values ranging from 6  
137 to 10 (pH 6 - 8: 5 mM phosphate buffer; pH 9 - 10: 5 mM borate buffer). Samples (1 mL)  
138 were collected at regular time intervals and stored at 4°C in the dark until analysis.  
139 Electronic absorption spectra of antiviral drugs at different pH values (see Fig. S2) were  
140 recorded with a UV-2600 UV-Vis Spectrophotometer (Shimadzu) using quartz-glass  
141 cuvettes (Hellma, Germany). Further details on determination of quantum yields using the  
142 *p*-nitroanisole (PNA)/pyridine(PYR) method<sup>20</sup> and related calculations are provided in  
143 section 1.6 of the SI.

144 Indirect phototransformation of antiviral drugs was investigated by the addition of specific  
145 quenchers to wetland water: *N,N*-dimethylaniline (DMA; 10 µM) was used to scavenge CO<sub>3</sub>-  
146 radicals<sup>10</sup>, sorbic acid (2.5 mM) was used to scavenge excited triplet states of the dissolved  
147 organic matter (<sup>3</sup>DOM\*)<sup>21</sup>, histidine (20 mM) was used to scavenge singlet oxygen (<sup>1</sup>O<sub>2</sub>)<sup>22</sup>  
148 and isopropyl alcohol (IPA; 26 mM) was used to scavenge •OH-radicals.<sup>23</sup> In addition,  
149 experiments with specific photosensitizers were conducted in ultrapure buffered water to  
150 determine reaction rate constants of antiviral drugs with individual reactive intermediates:  
151 For CO<sub>3</sub><sup>-</sup>, either NaNO<sub>3</sub>/NaHCO<sub>3</sub> or duroquinone/NaHCO<sub>3</sub> photosensitizer methods were  
152 used.<sup>24,25</sup> The excited triplet state photosensitizers 3-methoxyacetophenone (3MAP) and  
153 anthraquinone-2-sulfonate (AQ2S) served as proxies for <sup>3</sup>DOM\*.<sup>26</sup> Hydroxyl-radicals were  
154 generated by the irradiation of NaNO<sub>3</sub> solutions.<sup>27</sup> For <sup>1</sup>O<sub>2</sub> production, Rose Bengal was  
155 used as a photosensitizer.<sup>28</sup> To further verify the role of <sup>1</sup>O<sub>2</sub>, some experiments were  
156 performed in D<sub>2</sub>O. Reaction rate constants were either determined by competition kinetics  
157 or by comparing reaction rates of antiviral drugs with those of established photochemical  
158 probe compounds (experimental details and calculations are provided in section 1.5 and

159 1.7). For all indirect phototransformation experiments, the concentration changes of  
160 photochemical probe compounds and antiviral drugs during irradiations were determined  
161 by HPLC-UV. Experimental and analytical details, including comprehensive results are  
162 provided in the SI section 1.2.

163 Given the structural similarities of antivirals with DNA bases, additional irradiation  
164 experiments were performed with adenine, 2-amino adenosine, cytosine, cytidine, guanine,  
165 thymidine and thymine (SI section 2.1.1) to obtain further information about the  
166 photoreactive moieties in the molecules to aid the identification of transformation  
167 products.

168

169 *Identification of photo- and biotransformation products.* High resolution mass spectrometry  
170 (HR-MS; LTQ Orbitrap Velos, Thermo Scientific, Bremen, Germany) was used to conduct  
171 accurate MS and MS/MS analysis of transformation products of antiviral drugs. To this end,  
172 experiments at elevated concentrations (40  $\mu\text{M}$ ) were used. The LTQ Orbitrap Velos was  
173 coupled to a Thermo Scientific Accela liquid chromatography system (Accela pump and  
174 autosampler). HR-MS was conducted in the positive electrospray ionization (ESI) mode. To  
175 obtain information on the chemical structure of the TPs,  $\text{MS}^n$  fragmentation experiments  
176 were conducted using data-dependent acquisition. Further information on the applied  
177 setup and data dependent acquisition parameters can be found in the SI (section 1.3).  
178 Product formation of antiviral drugs in laboratory experiments was determined by liquid  
179 chromatography tandem mass spectrometry (LC/MS/MS). Details are provided in the SI  
180 (section 1.4).

181

182 *Combined bio- and photodegradation experiments.* The fate of antiviral drugs in the  
183 presence of sunlight and microorganisms was investigated over a 72 h period in the  
184 laboratory. Black-painted glass beakers (250mL) were filled with 180 mL of wetland water  
185 and 20 mL of freshly collected biomat material from the bottom of the Discovery Bay open-  
186 water unit process wetland. The experimental setup was the same as described above for  
187 photochemical experiments, but with three day/night cycles to simulate field conditions (8  
188 h of daily irradiation followed by 16 h in the darkness; 72 h total). Antiviral drugs were  
189 added individually at concentrations of 0.5  $\mu\text{M}$  to ensure detection of both parent antiviral



190 compounds and their transformation products. Samples were collected at regular time  
191 intervals and stored at 4°C in the dark prior to LC/MS/MS analysis, which occurred within  
192 24 h. Further details about the analytical method can be found in the SI.

193

## 194 **Results and Discussion**

### 195 *Phototransformation in wetland water*

196 Phototransformation of the five investigated antiviral drugs in wetland water followed  
197 first-order kinetics ( $r^2 \geq 0.98$ ; Figure S4-S8). In native wetland water (pH 8.9), the fastest  
198 phototransformation was observed for abacavir ( $k_{\text{obs}} = 0.52 \pm 0.06 \text{ h}^{-1}$ ), zidovudine ( $k_{\text{obs}} =$   
199  $0.09 \pm 0.002 \text{ h}^{-1}$ ) and emtricitabine ( $k_{\text{obs}} = 0.03 \pm 0.002 \text{ h}^{-1}$ ) whereas the transformation of  
200 acyclovir and lamivudine were significantly slower ( $k_{\text{obs}} = 0.012 \pm 0.001 \text{ h}^{-1}$  and  $0.011 \pm$   
201  $0.001 \text{ h}^{-1}$ , respectively) (Figure 2). No degradation of antiviral drugs in wetland water  
202 occurred in the dark indicating that their removal was solely attributable to photochemical  
203 processes. Photosynthetic activity leads to significant diurnal fluctuations of pH in open-  
204 surface wetlands.<sup>10</sup> Therefore, phototransformation kinetics of antiviral drugs in wetland  
205 water were also determined at pH 6.5 and pH 10 (Figure 2).

206

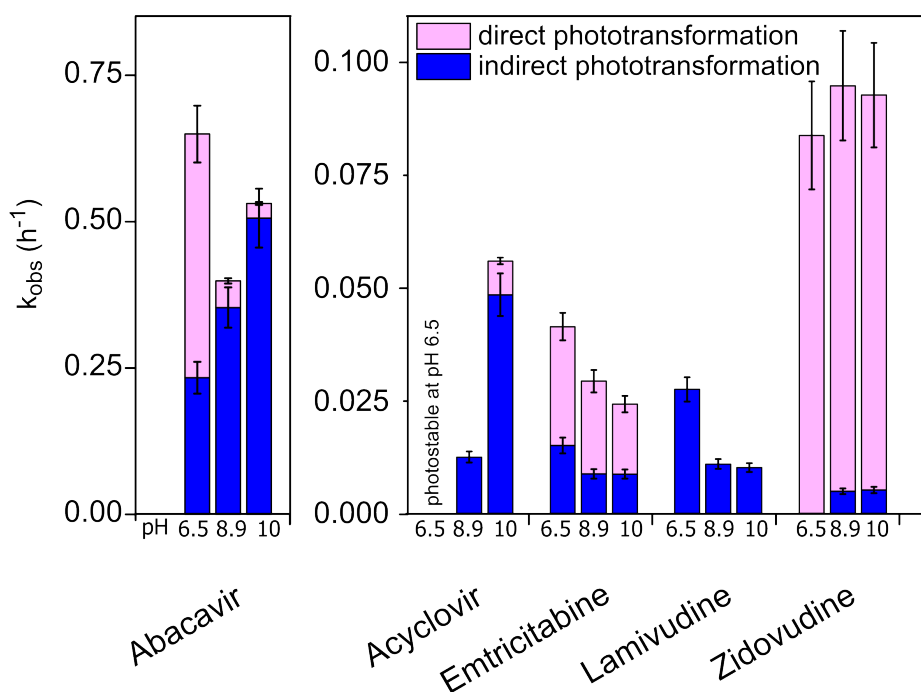


Figure 2. Phototransformation kinetics of antiviral drugs in experiments with

wetland water at different pH values and contribution of direct and indirect photolysis processes by comparison with results obtained in ultrapure water. Data for wetland water are corrected for light-absorption. Error bars show 95% confidence intervals.

207

208 Phototransformation of abacavir in wetland water increased when the pH value was  
209 adjusted to 6.5 or 10. This can be attributed to a higher contribution of direct photolysis  
210 due to higher quantum yields at lower pH values (i.e.,  $\Phi_{app}$  is 4.2 to 11.4 times higher  
211 between pH 6 – 8, compared to pH 9 and 10, SI Table S5) and faster indirect photolysis at  
212 higher pH values. Comparison of transformation kinetics with results obtained in ultrapure  
213 water revealed the dominance of indirect photodegradation processes at pH 8.9 and 10,  
214 whereas direct photolysis was more important at pH 6.5. The addition of sorbic acid and  
215 histidine significantly reduced phototransformation rates of abacavir in wetland water  
216 (Fig. S4). Although interpretation of results from experiments with scavengers requires  
217 caution,<sup>29</sup> these results suggest the involvement of  $^3DOM^*$  and  $^1O_2$  in the photochemical fate  
218 of this compound. This was also supported by experiments with specific singlet oxygen and  
219 excited triplet state sensitizers (see below). Negligible removal of the structural analogues  
220 adenine and 2-amino-adenosine further indicated that the photolability of abacavir can be  
221 attributed to the cyclopropyl-moiety (see SI section 2.1.1).

222 Rates of phototransformation of zidovudine were not affected by changes in pH.  
223 Comparison with reaction rates in both ultrapure water and wetland water in the presence  
224 of scavengers revealed the dominance of direct photolysis (Fig. S5). Similar to abacavir,  
225 comparison with the depletion of structural analogues thymine and thymidine indicated  
226 that the azide moiety was responsible for the observed photoreactivity of zidovudine as  
227 both analogues showed no removal when exposed to light (see SI section 2.1.1).

228 Phototransformation rates of acyclovir in wetland water increased with increasing pH.  
229 Comparison with results from ultrapure water revealed that removal at pH 8.9 was solely  
230 due to indirect photolysis, whereas at pH 10 direct photolysis was also important.  
231 Significantly reduced rates of acyclovir phototransformation in the presence of histidine  
232 and sorbic acid indicated the importance of  $^1O_2$  and  $^3DOM^*$  to indirect photolysis (Fig. S6).  
233 In contrast to abacavir and zidovudine, phototransformation kinetics were similar to those

234 observed for the structural analogue guanine (SI Fig. S15). Thus, phototransformation of  
235 acyclovir can be attributed primarily to the guanine moiety.

236 For lamivudine and emtricitabine, phototransformation kinetics in wetland water  
237 decreased with increasing pH. No removal of lamivudine was observed in ultrapure water  
238 indicating that its removal was entirely attributable to indirect photolysis. Higher  
239 phototransformation rates of emtricitabine relative to lamivudine further indicated the  
240 strong influence of the fluorine atom for emtricitabine's photolability. The presence of the  
241 fluorine substituent led to greater light absorption at 300-320 nm (SI Fig. S2). Even though  
242 the absorption spectrum of emtricitabine did not change with pH, the quantum yield  
243 steadily decreased with increasing pH (Table S5). Phototransformation of lamivudine in  
244 wetland water was fully inhibited by sorbic acid, histidine and IPA but was unaltered in the  
245 presence of DMA (Fig. S7). This indicates the importance of  $^3\text{DOM}^*$ ,  $^1\text{O}_2$  and OH-radicals for  
246 its indirect phototransformation. For emtricitabine, phototransformation rates in wetland  
247 water were only affected by IPA and sorbic acid (Fig. S8), suggesting that reactions with  $^1\text{O}_2$   
248 are less important for this compound. The high photostability of its associated DNA base  
249 cytosine and nucleotide cytidine revealed the importance of structural modifications (thiol  
250 group (both compounds) and fluorine (emtricitabine) to the observed photodegradation.

251

252 Additional experiments with individual reactive species revealed second-order reaction  
253 rates with  $\cdot\text{OH}$  at or above (abacavir, zidovudine) diffusion controlled rates ranging from  
254  $5 \cdot 10^9$  to  $1.1 \cdot 10^{11} \text{ M}^{-1}\text{s}^{-1}$  (Table 1). Antiviral compounds were reactive with  $\text{CO}_3^{\cdot-}$ , at rates  
255 between  $1.2 \cdot 10^6$  and  $1.2 \cdot 10^9 \text{ M}^{-1}\text{s}^{-1}$ , while only abacavir ( $1.2 \cdot 10^9 \text{ M}^{-1}\text{s}^{-1}$ ) and acyclovir  
256 ( $1.2 \cdot 10^7 \text{ M}^{-1}\text{s}^{-1}$ ) reacted with  $^1\text{O}_2$ . With the exception of abacavir, no depletion of antiviral  
257 compounds was observed in the presence of the model triplet photosensitizer 3MAP.  
258 However depletion of all compounds was observed in the presence of AQ2S at rates similar  
259 to or higher than the reference probe compound TMP, indicating selective reactivity with  
260 excited triplet states. Comparison of measured and predicted rate constant for antivirals  
261 under wetland conditions (obtained by multiplication of steady-state concentrations of  
262 reactive species measured in wetland water with measured second-order reaction rate  
263 constants of antivirals with  $^1\text{O}_2$ ,  $\cdot\text{OH}$  and  $\cdot\text{CO}_3^-$ ) were in good agreement, indicating  
264 reasonable results.

265

266

267

Table 1. Quantum yields (pH 9) and apparent second-order reaction rate constants of indirect phototransformation of antiviral drugs via reaction with  $^1\text{O}_2$ ,  $\cdot\text{OH}$ ,  $\cdot\text{CO}_3^-$  and excited triplet states (given relative to the degradation of the  $^3\text{Sens}^*$  probe compound TMP). Quantum yields of antiviral drugs at pH 6-8 and pH 10 can be found in SI Table S5.

	[M Es <sup>-1</sup> ]	[M <sup>-1</sup> s <sup>-1</sup> ]				[-]	
	$\Phi_{\text{app}(300-400\text{nm})}$ (pH 9)	$^1\text{O}_2$	$\cdot\text{OH}$	$\cdot\text{CO}_3^-$ ( $\text{NO}_3^- + \text{HCO}_3^-/\text{CO}_3^{2-}$ )	$\cdot\text{CO}_3^-$ (DQ)	$^3\text{SENS}^*$ (AQ2S)	$^3\text{SENS}^*$ (MAP)
<b>Abacavir</b>	0.014 (±0.003)	$1.2 \times 10^9$ (± 18%)	$1.1 \times 10^{11}$ (± 3%)	$1.2 \times 10^9$ (± 4%)	<sup>a</sup>	4.88	13.5
<b>Zidovudine</b>	0.45 (±0.15)	n.d.	$1.3 \times 10^{10}$ (± 2%)	$2.4 \times 10^6$ (± 5%)	$1.3 \times 10^6$ (± 4%)	0.62	n.d.
<b>Acyclovir</b>	0.01 (±0.005)	$1.2 \times 10^7$ (± 25%)	$5.0 \times 10^9$ (± 2%)	$1.2 \times 10^8$ (± 2%)	$6.3 \times 10^7$ (± 4%)	0.08	n.d.
<b>Emtricitabine</b>	0.016 (±0.005)	n.d.	$9.3 \times 10^9$ (± 2%)	$3.0 \times 10^6$ (± 4%)	$4.3 \times 10^6$ (± 12%)	2.03	n.d.
<b>Lamivudine</b>	n.d.	n.d.	$9.2 \times 10^9$ (± 1%)	$1.2 \times 10^6$ (± 3%)	$1.7 \times 10^6$ (± 3%)	1.86	n.d.

268 n.d.: not detected above level of uncertainty; <sup>a</sup> not applicable due to reaction of abacavir with DQ in the dark

269

### 270 Comparison of photo- vs biotransformation rates

271 Dark experiments conducted with wetland water in the presence of biomat material  
 272 indicated that biotransformation rates varied considerably among antiviral drugs.  
 273 Biotransformation half-life times ( $t_{1/2,\text{bio}}$ ) ranged from 74 h for acyclovir to 500 h (21 d) for  
 274 emtricitabine (Fig. 3; Fig. S13). Under typical wetland treatment conditions (i.e., hydraulic  
 275 retention times of 2-3 days), significant biological attenuation of acyclovir and abacavir is  
 276 expected whereas removal of the other antiviral drugs via microbial processes is unlikely  
 277 to be important. Comparison of transformation rates of antiviral drugs in the dark to those  
 278 observed in irradiated wetland water indicated that phototransformation processes were  
 279 dominant for abacavir, zidovudine and emtricitabine, while for acyclovir and lamivudine  
 280 biotransformation was similar or more important than photolysis during typical  
 281 summertime conditions (Fig. 3).

282

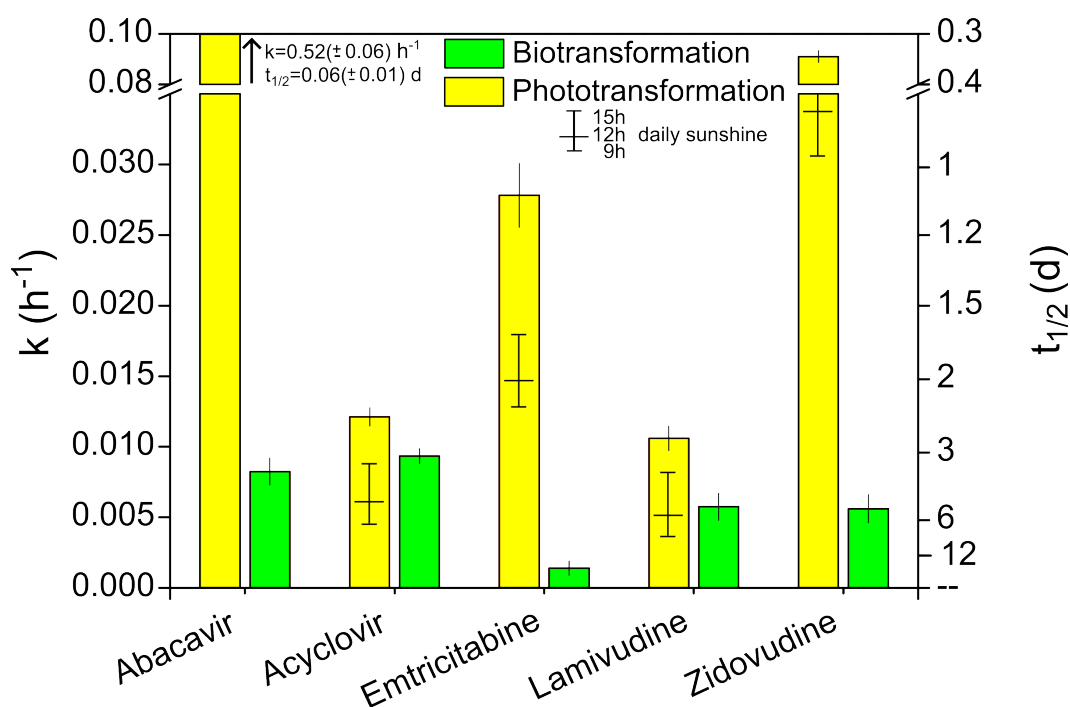


Figure 3. Photo- and biotransformation rate constants  $k$  ( $\text{h}^{-1}$ ) and associated half-life time  $t_{1/2}$  (d) of antiviral drugs in laboratory experiments. Small bars within phototransformation columns indicate half-life times based on daily sunshine hours (9-15 hours). For the determination of biodegradation half-life times, experiments were conducted in the presence of the biomat in the dark. Error bars represent 95% confidence intervals obtained from linear regressions.

283

#### 284 Transformation of abacavir

285 HRMS analysis indicated that four primary transformation products (TP318, TP288, TP284  
 286 and TP246) were formed during photolysis of abacavir in wetland water (SI section 2.2;  
 287 Table S7). In agreement with results obtained for the structural analogues 2-amino-  
 288 adenosine and adenine, fragmentation patterns of TP318, TP288 and TP246 revealed that  
 289 the cyclopropylamine moiety was the main site of reaction, leaving the 2-amino-adenine  
 290 (fragments:  $m/z$  151.073, 134.046 and 109.051) and the 2-cyclopenten-1-methanyl  
 291 moieties (fragments:  $m/z$  95.353 and 79.054) unaltered.

292 Exact mass calculations of TP318 showed addition of two oxygen atoms to the cyclopropyl  
 293 moiety ( $\Delta m +31.9898$  Da). Results from MS<sup>2</sup> experiments were consistent with the scission  
 294 of the cyclopropyl ring and the presence of a terminal hydroxyl group, as indicated by the  
 295 cleavage of H<sub>2</sub>O and CH<sub>2</sub>O.

296 For TP288, MS data suggested modification of the cyclopropyl moiety via loss of one carbon  
 297 atom and the addition of one oxygen atom, leading to the formation of an acetamide,

298 whereas TP246 was formed via cleavage of the cyclopropyl ring. The chemical structure of  
299 TP246 was confirmed by comparison with a commercially available reference standard.  
300 The exact mass and fragmentation pattern of TP284 was consistent with loss of two  
301 protons from either the cyclopropylamine or the 2-amino-adenosine moiety (fragments  
302  $m/z$  149.069 and 189.088 instead of  $m/z$  151.073 and 191.104 compared to abacavir and  
303 the other TPs). Considering the high photolability of the cyclopropyl moiety, these  
304 structural changes were most likely due to the formation of a cyclopropylimine.  
305 To assess the relative importance of direct and different indirect photolysis processes for  
306 formation of the observed abacavir transformation products, their formation was  
307 investigated in buffered water (direct photolysis only), wetland water (direct and indirect  
308 photolysis), and wetland water in the presence of different reactive intermediate  
309 scavengers. The results revealed that both direct and indirect photolysis of abacavir  
310 produced the same suite of TPs at similar relative concentrations, despite the fact that the  
311 disappearance of the parent compound was significantly accelerated in the presence of  
312 DOM and individual reactive intermediates (Fig. S17 & S18). Similar results have been  
313 reported for irgarol, an algaecide that is structurally similar to abacavir, suggesting that the  
314 cyclopropylamine moiety is the main site of reaction under all conditions.<sup>30</sup>  
315 Photodegradation experiments in buffered ultrapure water with different optical filters  
316 indicated that wavelengths below 320 nm preferentially led to cleavage of the cyclopropyl  
317 moiety (TP246), whereas wavelengths above 320 nm (UV-A & visible light) led to scission  
318 of the cyclopropyl ring followed by partial oxidation (TP318) (Fig. S19).  
319 These findings suggest that phototransformation of abacavir is initiated by a one-electron  
320 oxidation of the cyclopropylamine moiety, leading to the formation of a  
321 cyclopropylaminium radical cation,<sup>31,32</sup> followed by subsequent reactions resulting in the  
322 formation of various products. Interestingly, this phenomenon has also been utilized for  
323 the investigation of electron-hopping in DNA by modifying guanine and adenine with  
324 cyclopropyl moieties.<sup>33,34</sup> Due to the instability of the initially formed closed ring radical  
325 cation, the modification results in rapid cyclopropyl ring-opening as well as 1,2-hydrogen  
326 migration, leading to the formation of an ionized allylamine.<sup>31,35</sup> Scission of the ring is  
327 followed either by a complete cleavage of the cyclopropyl moiety (TP246) or reaction of the  
328 ring opened radical cation with  $H_2O/O_2$ .<sup>33,35</sup> In the latter case, electron release from the

329 carbon centered radical followed by hydrolysis leads to the formation of a 3-  
330 hydroxypropanaminium cation<sup>36</sup> and subsequent addition of water results in the formation  
331 of the 3-hydroxypropanamide (TP318). In our system, TP288 is formed by photolytic  
332 cleavage of the hydroxymethyl group which leads to the formation of the acetamide  
333 product.<sup>36,37</sup> TP284 was most likely formed via H-atom abstraction, resulting in the  
334 formation of a neutral cyclopropyl radical followed by an electron transfer reaction and/or  
335 hydrolysis and elimination of water even though this reaction has only been shown to be  
336 catalyzed by enzymes so far.<sup>38,39</sup>

337

338 Experiments with biomat material in the dark to determine the relative importance of  
339 biotransformation reactions indicated that microbial transformation of abacavir mainly  
340 occurred via oxidation of the primary alcohol group of the 2-cyclopenten-1-  
341 hydroxymethyl side chain to produce the corresponding carboxylic acid (abacavir  
342 carboxylate, Fig. S13). This was consistent with previous experiments conducted with  
343 mixed liquor suspended solids from an activated sludge treatment plant.<sup>40</sup>

344

345 When abacavir was exposed simultaneously to light and microorganisms (Fig. 4), a rapid  
346 loss of the compound was observed during the first 8-hour light period (i.e., the initial  
347 concentration decreased by approximately 90 %). For the next 16 hours (i.e., the dark  
348 period) abacavir removal was significantly slower. When the light was turned back on,  
349 nearly all remaining abacavir disappeared. As expected, the light-induced transformation of  
350 abacavir gave rise to the four photo-TPs described above (middle panel of Fig. 4). The  
351 concentrations of these photo-TPs decreased by approximately 25% over the next 2.5 days,  
352 indicating that further transformation took place, either via photolytic or microbial  
353 processes.

354 Additional biodegradation experiments with the four photo-TPs of abacavir revealed that  
355 biotransformation occurs at the same moiety as observed for the parent compound, leading  
356 to the corresponding carboxylates (TP246 carboxylate, TP284 carboxylate, TP288  
357 carboxylate and TP318 carboxylate; Fig. S20). Exact mass data and fragmentation patterns  
358 of bio-photo TPs determined by HRMS analysis are included in section 2.2 of the SI.  
359 Consequently, the observed decrease in concentration of photo-TPs shown in the middle

360 panel of Fig. 4 was mainly attributable to biotransformation, leading to a steady formation  
361 of carboxylate photo-TPs (bottom panel of Fig. 4). Faster transformation rates of abacavir  
362 photo-TPs observed during irradiation periods may have been attributable to enhanced  
363 biotransformation due to elevated oxygen concentrations or elevated pH values that  
364 occurred when photosynthetic microbes in the biomat were active. Differences in  
365 biotransformation rates of TP246, TP284, TP288 and TP318, compared to abacavir (Fig.  
366 S14), indicate that alteration of chemical structure influences biotransformation kinetics,  
367 e.g. by affecting enzyme binding affinities or steric properties. Light-exposure of abacavir  
368 carboxylate formed in the dark led to its phototransformation, ultimately yielding the same  
369 photo-TPs as abacavir (bottom panel of Fig. 4). Considering that abacavir is already  
370 transformed extensively to abacavir carboxylate in activated sludge treatment,<sup>40</sup> a rapid  
371 elimination of both compounds can be expected in open-water unit process wetlands. In  
372 contrast to biotransformation reactions, similar phototransformation kinetics were  
373 observed for abacavir and abacavir carboxylate (Fig. S12). TP246 carboxylate was  
374 identified as the main product that accumulates over time because it is not susceptible to  
375 further reactions.



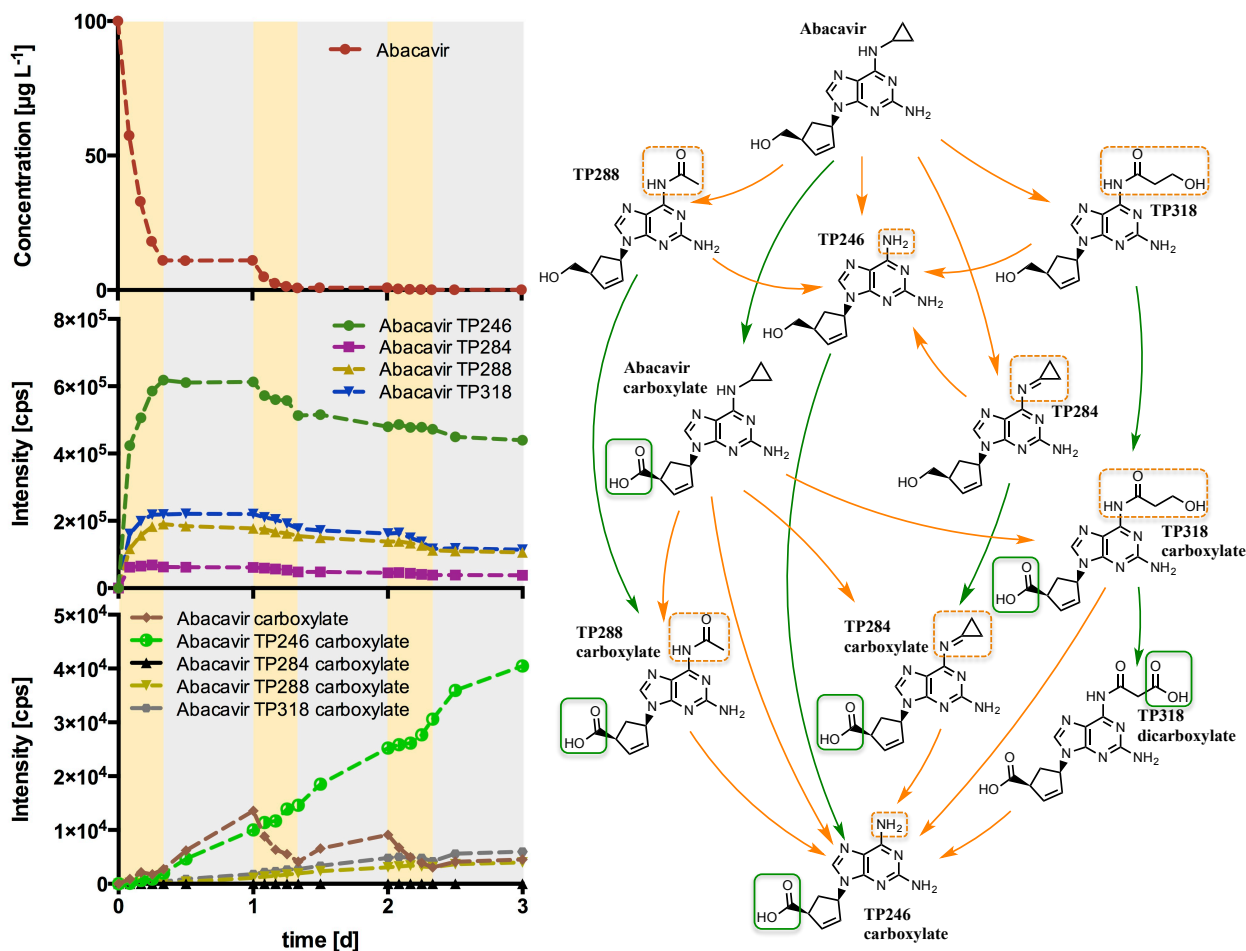


Figure 4. Transformation of abacavir (left, top) and resulting formation of photo-TPs (left, middle) and bio- / bio-photo-TPs (left, bottom)) as well as proposed transformation pathway (right) in combined in 3 day experiments in the presence of biomat with 8 hours of daily irradiation. In the transformation pathway, photo- and biotransformation reactions and structural changes in the molecules are indicated in orange and green, respectively.

376

### 377 Transformation of acyclovir

378 In contrast to abacavir, the transformation of acyclovir was dominated by microbial  
 379 processes (Fig. 5), with biotransformation resulting in the formation of acyclovir  
 380 carboxylate, which was not susceptible to further microbial transformation. These results  
 381 are consistent with previous biotransformation experiments conducted with acyclovir in  
 382 sewage sludge.<sup>41</sup>

383 In the absence of biomat material, exposure of wetland water to simulated sunlight  
 384 resulted in formation of two main photo-TPs (*i.e.*, TP257 and TP223). HRMS analysis  
 385 indicated that TP257 contains two additional oxygen atoms on the guanine moiety, as

386 evidenced by the detection of fragment m/z 184 instead of m/z 152 (Table S8; Fig. S16).  
387 Photosensitized degradation of guanine and guanosine occurs by reaction with excited  
388 triplet states,  $^1\text{O}_2$ ,  $\cdot\text{OH}$  or  $\cdot\text{CO}_3^-$ .<sup>42,43</sup> The main product of the reaction of guanine with  $^1\text{O}_2$  has  
389 been identified as spiroiminodihydantoin.<sup>44-46</sup> To assess the role of  $^1\text{O}_2$  in the  
390 phototransformation of acyclovir in wetland water, experiments were conducted in both  
391  $\text{H}_2\text{O}$  and  $\text{D}_2\text{O}$  in the presence of the  $^1\text{O}_2$  sensitizer Rose Bengal (Fig. 5). Lifetimes of  $^1\text{O}_2$  in  
392  $\text{D}_2\text{O}$  are more than an order of magnitude higher than in  $\text{H}_2\text{O}$  <sup>39</sup> and faster transformation  
393 of acyclovir in  $\text{D}_2\text{O}$  confirmed the role of  $^1\text{O}_2$  in the indirect photolysis of acyclovir. In  
394 addition, the yield of TP257 increased in  $\text{D}_2\text{O}$ . Due to its photochemical properties,  
395 acyclovir is likely to undergo self-sensitization via photoexcitation and subsequent formation  
396 of  $^1\text{O}_2$  as shown for guanine and guanosine.<sup>48-50</sup> For the second acyclovir photo-TP (TP223),  
397 HRMS analysis indicated the loss of two protons, most likely from the side chain, as  
398 evidenced by the detection of fragments m/z 152, 135 and 110, suggesting that the guanine  
399 moiety remained unchanged (Table S8). Additional information obtained from the  
400 fragmentation of the side chain was inconclusive but indicated oxidation of the terminal  
401 alcohol to the corresponding aldehyde via reaction with  $\cdot\text{OH}$ .<sup>51</sup>  
402 Results from the 72h simulated sunlight experiments conducted in the presence of the  
403 biomat revealed a steady decrease of acyclovir during light and dark periods, indicating the  
404 dominance of biotransformation processes (Fig. 5b). However, biotransformation of  
405 acyclovir was significantly faster in the sunlight experiments compared to dark controls  
406 (Fig. 5a&b) suggesting that the higher oxygen concentrations and the elevated pH values  
407 that occurred when microorganisms in the biomat were undergoing photosynthesis played  
408 a role in the biotransformation processes.<sup>10</sup> In the presence of simulated sunlight,  
409 production of the two phototransformation products (i.e., TP257 and TP224) was  
410 observed. No significant removal of TP257 was detected during dark periods, suggesting  
411 limited biotransformation via oxidation of the terminal hydroxyl-group of the side chain.  
412 Although the exact reason for this is unknown, a plausible explanation is that the structural  
413 modifications of the guanine core moiety prevented enzymatic oxidation of TP257. In  
414 contrast, concentrations of TP223 decreased in the dark. For the biotransformation  
415 product (i.e., acyclovir carboxylate), increasing concentrations were only observed during  
416 dark periods, whereas its concentration decreased upon exposure to sunlight. This

417 indicates that the compound was transformed further by photolytic processes, most likely  
 418 via the same mechanisms as acyclovir. This was confirmed by additional irradiation  
 419 experiments with acyclovir carboxylate in wetland water (results not shown).  
 420

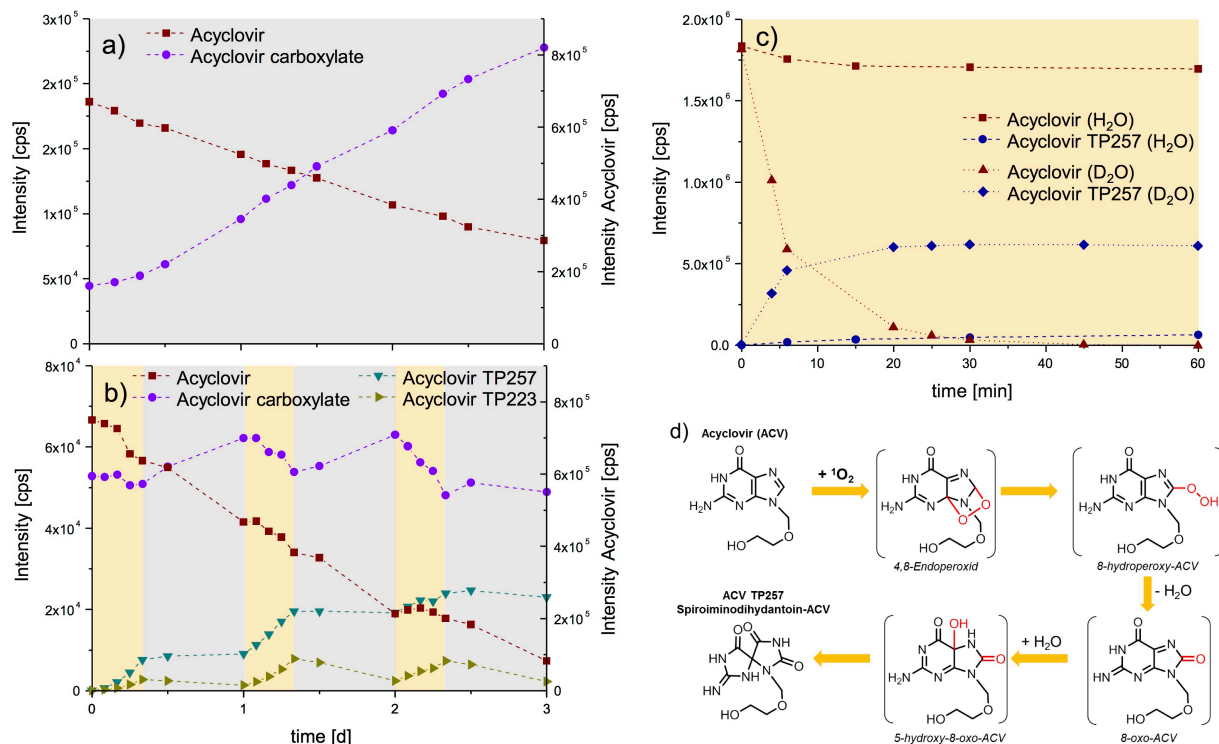


Figure 5. Transformation of acyclovir in the presence of biomat in the dark (a) in combined photo- and biotransformation experiments (b), as well as formation of TP257 via reaction of acyclovir with <sup>1</sup>O<sub>2</sub> in D<sub>2</sub>O and H<sub>2</sub>O using Rose Bengal as photosensitizer (c) and its proposed phototransformation pathway (d). The occurrence of acyclovir carboxylate at t<sub>0</sub> in (a) and (b) is due to its emission by the WWTP that feeds the wetland.

421  
 422 Transformation of zidovudine, lamivudine and emtricitabine  
 423 MS spectra of the phototransformation products of emtricitabine, lamivudine and  
 424 zidovudine indicated structural changes at different positions on the molecules (Table S9-  
 425 S11). For lamivudine and emtricitabine, HRMS analysis revealed oxidation of the riboside  
 426 moiety (lamivudine TP245 and emtricitabine TP263), most likely via S-oxidation. This was  
 427 confirmed by comparison with commercially available reference standards. Addition of  
 428 H<sub>2</sub>O to the 5-fluoro-cytosine moiety was observed for emtricitabine (emtricitabine TP265).  
 429 Experiments conducted with the fluorine-free analogue lamivudine illustrate the  
 430 importance of fluorine substitution: the F-moiety increases the light absorbance at

431 wavelengths > 300 nm (Fig. S2) for emtricitabine and leads to faster photodegradation  
432 (Figure 1, Table S5). Emtricitabine TP265 was formed via hydration of the double bond of  
433 the 5-fluorocytosine moiety, yielding a hydroxyl-group at position C6. For zidovudine,  
434 observed phototransformations were mainly attributable to the photolability of the azido  
435 moiety. Formation of zidovudine TP239 can be explained by cleavage of N<sub>2</sub>, yielding a  
436 nitrene intermediate, which reacts further via intramolecular C-H insertion to an  
437 aziridine.<sup>52,53</sup> Subsequent nucleophilic attack of the aziridine by water leads to the  
438 hydroxylation of the C atom in  $\beta$ -position or the formation of a hydroxylamine (zidovudine  
439 TP257).<sup>52,54</sup> Results from HRMS analysis of zidovudine TP221 were inconclusive but  
440 indicated cleavage of N<sub>2</sub> and H<sub>2</sub>O from the furanosyl moiety.

441 In addition, photolytic cleavage of the nitrogen-carbon bond between the DNA base  
442 moieties and the riboside analogue side chains was observed for all three compounds,  
443 resulting in formation 5-fluoro-cytosine (emtricitabine TP129), cytosine (lamivudine  
444 TP111) and thymine (zidovudine TP126). None of these TPs were detected in sunlight  
445 experiments in the presence of biomat (Fig. S21-22), indicating that they were rapidly  
446 transformed, most likely via microbial processes. For zidovudine, this was confirmed by  
447 additional biodegradation experiments with the photo-TPs (i.e., thymine, TP239, TP257),  
448 showing the rapid elimination of thymine (Fig. S22). Considering the importance of both  
449 thymine and cytosine as DNA building blocks, it is likely that they were incorporated into  
450 the microbial biomass. The fate of 5-fluorocytosine remains unclear.

451 Similar to abacavir and acyclovir, biotransformation of emtricitabine, lamivudine and  
452 zidovudine was shown to result in the formation of carboxylated TPs via oxidation of the  
453 terminal alcohol as observed previously for abacavir and acyclovir (Fig. S13). As  
454 carboxylated TPs are expected to follow the same phototransformation mechanisms as the  
455 parent compounds, the interactions of photo- and biotransformation reactions is likely to  
456 result in their complete elimination via mineralization and/or microbial uptake (Fig. 6).

457

458

459

460

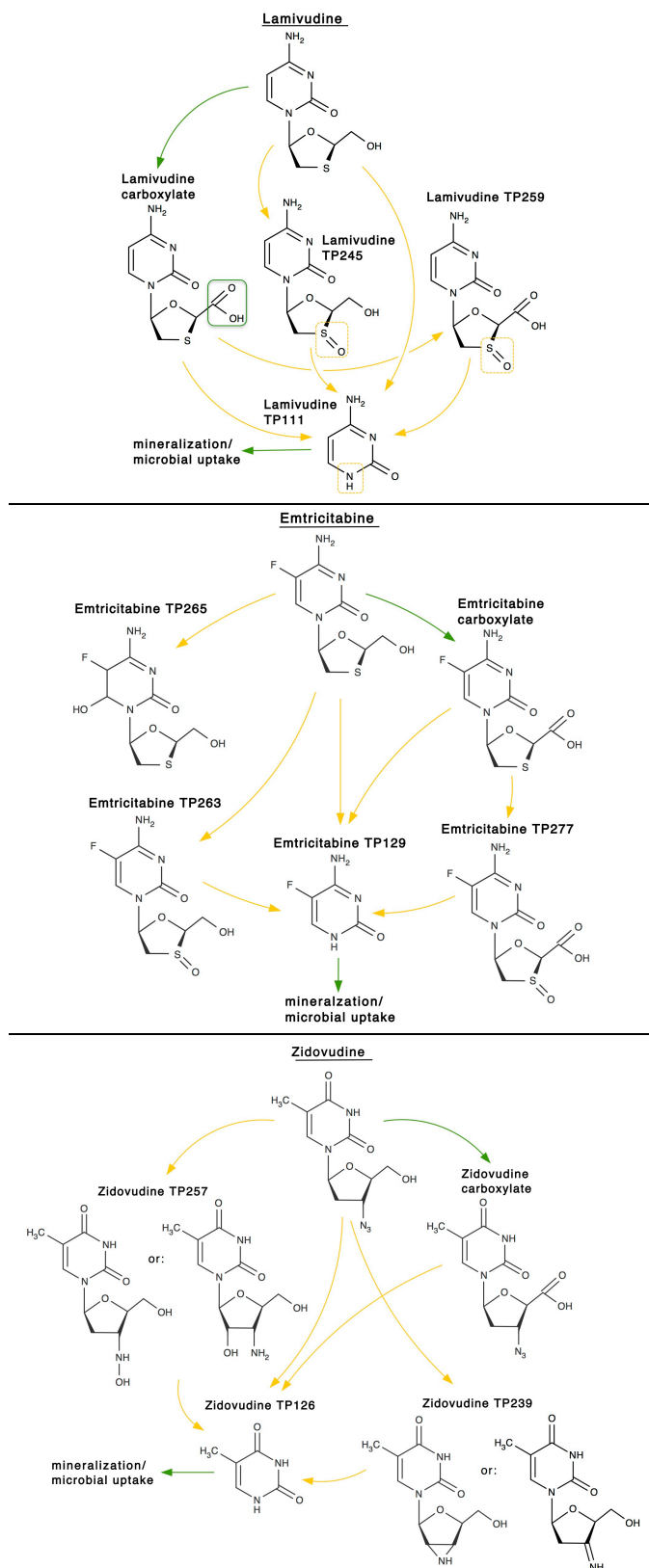


Figure 6. Proposed photo- and biodegradation pathway of lamivudine (top), emtricitabine (middle) and zidovudine (bottom) in open-water wetland cells. Orange and green

arrows indicate photo- and biotransformation reactions,  
respectively.

461

462 *Environmental implications*

463 The differences between kinetics and transformation product formation in the presence  
464 and absence of the biomat highlight the complexity of transformation reactions that lead to  
465 the removal of trace organic contaminants in open water unit process wetlands and other  
466 sunlit waters. Attempts to predict the environmental fate of organic contaminants in these  
467 systems requires an understanding of both processes as well as their potential interactions.  
468 Identification of TPs showed that bio- and phototransformation reactions took place at  
469 different positions of the antiviral molecules. Phototransformation of biodegradation  
470 products was found to occur at the same location as in the parent compound. As a result,  
471 mechanisms and kinetics were similar to those observed for parent antiviral compounds.  
472 This is important because carboxylate biodegradation products are typically present in  
473 much higher concentrations in biological treated wastewater compared to parent  
474 compounds.<sup>40</sup> In contrast, biodegradation kinetics of phototransformation products of  
475 antiviral drugs differed substantially from that observed for the parent compound even  
476 though the site of enzymatic oxidation did not change. This can be explained by differences  
477 in enzyme affinities and steric hindrance. For example, phototransformation of acyclovir  
478 created a transformation product (TP257) that was not susceptible to biotransformation  
479 by microorganisms that could oxidize the parent compound in the dark.

480 Combining kinetic studies with investigations of transformation product formation  
481 provides a better understanding of mechanisms relevant for the removal of trace organic  
482 contaminants in sunlit waters. By conducting biotransformation studies in the presence  
483 and absence of light it is possible to assess interactions between transformation processes  
484 and the likelihood that complete mineralization of trace organic contaminants will occur.  
485 These data also suggest that relative ratios of antiviral compounds and their  
486 transformation products might be useful as *in situ* probes to assess the relative importance  
487 of microbial and photochemical transformation pathways. This study highlights the need to  
488 consider the formation of different transformation products in sunlit and light-shaded  
489 systems and the possibility of using knowledge of the reactivity of specific moieties in

490 chemical fate assessment. Considering the variety of formed transformation products,  
491 there is a need for appropriate risk assessment tools to assess potential adverse effects of  
492 transformation products with unknown toxicities on aquatic ecosystems. Additional field  
493 studies may further confirm these laboratory microcosm results and help to assess the  
494 suitability of the approach for determining the relative importance of individual  
495 transformation processes.

496

### 497 **Supporting Information**

498 Additional information on sample analysis, UV spectra of antiviral drugs,  
499 phototransformation kinetics plots, determination of indirect photolysis reaction rate  
500 constants, quantum yields, steady state concentrations of reactive intermediates in wetland  
501 water, experiments with DNA model compounds, MS<sup>n</sup> fragments of transformation  
502 products, formation and fate of abacavir photo-TPs by different reactive intermediates,  
503 results of combined bio- and phototransformation experiments with emtricitabine,  
504 lamivudine and zidovudine is available free of charge via the Internet at  
505 <http://pubs.acs.org>.

506

### 507 **Acknowledgement**

508 C.P. was supported by a postdoctoral scholarship of the German Academic Exchange  
509 Service (DAAD), J.W. by a scholarship of the Swiss National Science Foundation (PBEZP2-  
510 142887). Financial support by the Engineering Research Center for Reinventing the  
511 Nation's Water Infrastructure (ReNUWIt) EEC-1028968, and TransRisk, funded by the  
512 German Ministry of Science and Education, is gratefully acknowledged.

513

### 514 **References**

- 515 (1) Burrows, H.DI; Canle, M.; Santaballa, J.A.; Steenken, S. Reaction pathways and  
516 mechanisms of photodegradation of pesticides. *J. Photoch. Photobio. B* **2002**, 67(2),  
517 71-108.
- 518 (2) Boreen, A.L.; Arnold, W.A.; McNeill, K. Photodegradation of pharmaceuticals in the  
519 aquatic environment: A review. *Aquat. Sci.* **2003**, 65(4), 320-341.
- 520 (3) Halling-Sorensen, B.; Nielsen, S.N.; Lanzky, P.F.; Ingerslev, F.; Lutzhof, H.C.H.;  
521 Jorgensen, S.E. Occurrence, fate and effects of pharmaceutical substances in the  
522 environment - A review. *Chemosphere* **1998**, 36(2), 357-394.

- 523 (4) Onesios, K.M.; Yu, J.T.; Bouwer, E.J. Biodegradation and removal of pharmaceuticals  
524 and personal care products in treatment systems: a review. *Biodegradation* **2009**,  
525 20(4), 441-466.
- 526 (5) Lam, M.W.; Mabury, S.A. Photodegradation of the pharmaceuticals atorvastatin,  
527 carbamazepine, levofloxacin, and sulfamethoxazole in natural waters. *Aquat. Sci.*  
528 **2005**, 67(2), 177-188.
- 529 (6) Chiron, S.; Minero, C.; Vione, D. Photodegradation processes of the antiepileptic drug  
530 carbamazepine, relevant to estuarine waters. *Environ. Sci. Technol.* **2006**, 40(19),  
531 5977-5983.
- 532 (7) De Laurentiis, E.; Chiron, S.; Kouras-Hadef, S., Richard, C.; Minella, M.; Maurino, V.;  
533 Minero, C.; Vione, D. Photochemical fate of carbamazepine in surface freshwaters:  
534 Laboratory measures and modeling. *Environ. Sci. Technol.* **2012**, 46(15), 8164-8173.
- 535 (8) Kaiser, E.; Prasse, C.; Wagner, M.; Broeder, K.; Ternes, T.A. Transformation of  
536 oxcarbazepine and human metabolites of carbamazepine and oxcarbazepine in  
537 wastewater treatment and sand filters. *Environ. Sci. Technol.* **2014**, 48(17), 10208-  
538 10216.
- 539 (9) Jasper, J.T.; Nguyen, M.T. Jones, Z.L.; Ismail, N.S.; Sedlak, D.L., Sharp, J.O.; Luthy, R.G.,  
540 Horne, A.J.; Nelson, K.L. Unit process wetlands for removal of trace organic  
541 contaminants and pathogens from municipal wastewater effluents. *Environ. Engin.*  
542 *Sci.* **2013**, 30(8), 421-436.
- 543 (10) Jasper, J.T.; Sedlak, D.L. Phototransformation of wastewater-derived trace organic  
544 contaminants in open-water unit process treatment wetlands. *Environ. Sci. Technol.*  
545 **2013**, 47(19), 10781-10790.
- 546 (11) Nguyen, M.T.; Silverman, A.I.; Nelson, K.L. Sunlight inactivation of MS2 coliphage in  
547 the absence of photosensitizers: Modeling the endogenous inactivation rate using a  
548 photoaction spectrum. *Environ. Sci. Technol.* **2014**, 48(7), 3891-3898.
- 549 (12) Silverman, A.I.; Nguyen, M.T.; Schilling, I.E.; Wenk, J.; Nelson, K.L. Sunlight  
550 inactivation of viruses in open-water unit process treatment wetlands: Modeling  
551 endogenous and exogenous inactivation rates. *Environ. Sci. Technol.* **2015**, 49(5),  
552 2757-2766.
- 553 (13) Jasper, J.T.; Jones, Z.L.; Sharp, J.O.; Sedlak, D.L. Biotransformation of trace organic  
554 contaminants in open-water unit process treatment wetlands. *Environ. Sci. Technol.*  
555 **2014**, 48(9), 5136-5144.
- 556 (14) Jasper, J.T.; Jones, Z.L.; Sharp, J.O.; Sedlak, D.L. Nitrate removal in shallow, open-  
557 water treatment wetlands. *Environ. Sci. Technol.* **2014**, 48(19), 11512-11520.
- 558 (15) Wood, T.P.; Duvenage, C.S.J.; Rohwer, E. The occurrence of anti-retroviral  
559 compounds used for HIV treatment in South African surface water. *Environ. Pollut.*  
560 **2015**, 199, 235-243.
- 561 (16) Peng, X.; Wang, C.; Zhang, K.; Wang, Z.F.; Huang, Q.X.; Yu, Y.Y.; Ou, W.H. Profile and  
562 behavior of antiviral drugs in aquatic environments of the Pearl River Delta, China.  
563 *Sci. Total Environ.* **2014**, 466, 755-761.
- 564 (17) Prasse, C.; Schluesener, M.P.; Schulz, R.; Ternes, T.A. Antiviral drugs in wastewater  
565 and surface waters: A new pharmaceutical class of environmental relevance?  
566 *Environ. Sci. Technol.* **2010**, 44(5), 1728-1735.



- 567 (18) Azuma, T.; Nakada, N.; Yamashita, N.; Tanaka, H. Synchronous dynamics of observed  
568 and predicted values of anti-influenza drugs in environmental waters during a  
569 seasonal influenza outbreak. *Environ. Sci. Technol.* **2012**, 46(23), 12873-12881.
- 570 (19) Wommack, K.E.; Colwell, R.R. Virioplankton: Viruses in aquatic ecosystems.  
571 *Microbiol. Mol. Biol. R.* **2000**, 64(1), 69-114.
- 572 (20) Dulin, D.; Mill, T. Development and evaluation of sunlight actinometers. *Environ. Sci.*  
573 *Technol.* **1982**, 16(11), 815-820.
- 574 (21) Grebel, J. E.; Pignatello, J. J.; Mitch, W. A. Sorbic acid as a quantitative probe for the  
575 formation, scavenging and steady-state concentrations of the triplet-excited state of  
576 organic compounds. *Water Res.* **2011**, 45(19), 6535-6544.
- 577 (22) Boreen, A.L.; Edhlund, B.L.; Cotner, J.B.; McNeill, K. Indirectphotodegradation of  
578 dissolved free amino acids: The contribution of singlet oxygen and the differential  
579 reactivity of DOM from various sources. *Environ. Sci. Technol.* **2008**, 42(15),  
580 5492-5498.
- 581 (23) Packer, J. L.; Werner, J.J.; Latch, D.E.; McNeill, K.; Arnold, W.A. Photochemical fate of  
582 pharmaceuticals in the environment: Naproxen, diclofenac, clofibrac acid, and  
583 ibuprofen. *Aquat. Sci.* **2003**, 65(4), 342-351.
- 584 (24) Vione, D.; Khanra, S.; Man, S.C.; Maddigapu, P.R.; Das, R.; Arsene, C.; Olariu, R.-I.;  
585 Maurino, V.; Minero, C. Inhibition vs. enhancement of the nitrate-induced  
586 phototransformation of organic substrates by the (OH)-O-center dot scavengers  
587 bicarbonate and carbonate. *Water Res.* **2009**, 43(18), 4718-4728.
- 588 (25) Canonica, S.; Kohn, T.; Mac, M.; Real, F.J.; Wirz, J.; Von Gunten, U. Photosensitizer  
589 method to determine rate constants for the reaction of carbonate radical with  
590 organic compounds. *Environ. Sci. Technol.* **2005**, 39(23), 9182-9188.
- 591 (26) Bedini, A.; De Laurentiis, E.; Sur, B.; Maurino, V.; Minero, C.; Brigante, M.; Mailhot, G.;  
592 Vione, D. Phototransformation of anthraquinone-2-sulphonate in aqueous solution.  
593 *Photochem. Photobio. S.* **2012**, 11(9), 1445-1453.
- 594 (27) Zepp, R.G.; Hoigne, J.; Bader, H. Nitrate-induced photooxidation of trace organic  
595 chemicals in water. *Environ. Sci. Technol.* **1987**, 21, 443-450.
- 596 (28) Burns, J.M.; Cooper, W.J.; Ferry, J.L.; King, D.W.; DiMento, B.P.; McNeill, K.; Miller, C.J.;  
597 Miller, W.L.; Peake, B.M.; Rusak, S.A.; Rose, A.L.; Waite, T.D. Methods for reactive  
598 oxygen species (ROS) detection in aqueous environments. *Aquat. Sci.* **2012**, 74(4),  
599 683-734.
- 600 (29) Maddigapu, P.R.; Bedini, A.; Minero, C.; Maurino, V., Vione, D.; Brigante, M.; Mailhot,  
601 G.; Sarakha, M. The pH-dependent photochemistry of anthraquinone-2-sulfonate.  
602 *Photochem. Photobio. Sci.* **2010**, 9(3), 323-330.
- 603 (30) Sakkas, V.A.; Lambropoulou, D.A.; Albanis, T.A. Photochemical degradation study of  
604 irgarol 1051 in natural waters: influence of humic and fulvic substances on the  
605 reaction. *J. Photoch. Photobio. A* **2002**, 147(2), 135-141.
- 606 (31) Bouchoux, G.; Alcaraz, C.; Dutuit, O.; Nguyen, M.T. Unimolecular chemistry of the  
607 gaseous cyclopropylamine radical cation. *J. Am. Chem. Soc.* **1998**, 120(1), 152-160.
- 608 (32) Cooksy, A.L.; King, H.F.; Richardson, W.H. Molecular orbital calculations of ring  
609 opening of the isoelectronic cyclopropylcarbinyl radical, cyclopropoxy radical, and  
610 cyclopropylaminium radical cation series of radical clocks. *J. Org. Chem.* **2003**,  
611 68(24), 9441-9452.

- 612 (33) Nakatani, K.; Dohno, C.; Saito, I. Design of a hole-trapping nucleobase: Termination  
613 of DNA-mediated hole transport at N-2-cyclopropyldeoxyguanosine. *J. Am. Chem.*  
614 *Soc.* **2001**, 123(39), 9681-9682.
- 615 (34) Shao, F.W.; O'Neill, M.A.; Barton, J.K. Long-range oxidative damage to cytosines in  
616 duplex DNA. *P. Natl. Acad. Sci. USA* **2004**, 101(52), 17914-17919.
- 617 (35) Qin, X.Z.; Williams, F. Electron-spin-resonance studies on the radical cation  
618 mechanism of the ring-opening of cyclopropylamines. *J. Am. Chem. Soc.* **1987**,  
619 109(2), 595-597.
- 620 (36) Paul, M.M.S.; Aravind, U.K.; Pramod, G.; Saha, A.; Aravindakumar, C.T. Hydroxyl  
621 radical induced oxidation of theophylline in water: a kinetic and mechanistic study.  
622 *Org. Biomol. Chem.* **2014**, 12(30), 5611-5620.
- 623 (37) Goutailler, G.; Valette, J.C.; Guillard, C.; Paisse, O.; Faure, R. Photocatalysed  
624 degradation of cyromazine in aqueous titanium dioxide suspensions: comparison  
625 with photolysis. *J. Photoch. Photobio. A* **2001**, 141(1), 79-84.
- 626 (38) Shaffer, C.L.; Morton, M.D.; Hanzlik, R.P. N-dealkylation of an N-cyclopropylamine by  
627 horseradish peroxidase. Fate of the cyclopropyl group. *J. Am. Chem. Soc.* **2001**,  
628 123(35), 8502-8508.
- 629 (39) Cerny, M.A.; Hanzlik, R.P. Cytochrome P450-catalyzed oxidation of N-benzyl-N-  
630 cyclopropylamine generates both cyclopropanone hydrate and 3-  
631 hydroxypropionaldehyde via hydrogen abstraction, not single electron transfer. *J.*  
632 *Am. Chem. Soc.* **2006**, 128(10), 3346-3354.
- 633 (40) Funke, J.; Prasse, C.; Ternes T.A. Identification and fate of transformation products of  
634 antiviral drugs formed during biological wastewater treatment (submitted).
- 635 (41) Prasse, C.; Wagner, M.; Schulz, R.; Ternes, T.A. Biotransformation of the antiviral  
636 drugs acyclovir and penciclovir in activated sludge treatment. *Environ. Sci. Technol.*  
637 **2011**, 45(7), 2761-2769.
- 638 (42) Cadet, J.; Douki, T.; Gasparutto, D.; Ravanat, J.L. Oxidative damage to DNA: formation,  
639 measurement and biochemical features. *Mutat. Res. - Fund. Mol. M.* **2003**, 531(1-2),  
640 5-23.
- 641 (43) Neeley, W.L.; Essigmann, J.M. Mechanisms of formation, genotoxicity, and mutation  
642 of guanine oxidation products. *Chem. Res. Toxicol.* **2006**, 19(4), 491-505.
- 643 (44) Cui, L.; Ye, W.; Prestwich, E.G.; Wishnok, J.S.; Taghizadeh, K.; Dedon, P.C.;  
644 Tannenbaum S.R. Comparative analysis of four oxidized guanine lesions from  
645 reactions of DNA with peroxyxynitrite, singlet oxygen and  $\gamma$ -radiation. *Chem. Res.*  
646 *Toxicol.* **2012**, 26(2), 195-202
- 647 (45) Luo, W.; Muller, J.G.; Rachlin, E.M.; Burrows, C.J. Characterization of  
648 spiroiminodihydroantoin as a product of one-electron oxidation of 8-oxo-7,8-  
649 dihydroguanosine. *Org. Lett.* **2000**, 2(5), 613-616.
- 650 (46) Cadet, J.; Douki, T.; Ravanat, J.L. Oxidatively generated damage to the guanine moiety  
651 of DNA: Mechanistic aspects and formation in cells. *Accounts Chem. Res.* **2008**, 41(8),  
652 1075-1083.
- 653 (47) Rodgers, M. A. J.; Snowden, P. T. Lifetime of  $O_2(1\Delta_g)$  in liquid water as determined by  
654 time-resolved infrared luminescence measurements. *J. Am. Chem. Soc.* **1982**,  
655 104(20), 5541-5543.

- 656 (48) Mohammad, T.; Morrison, H. Evidence for the photosensitized formation of singlet  
657 oxygen by UVB irradiation of 2'-deoxyguanosine 5'-monophosphate. *J. Am. Chem.*  
658 *Soc.* **1996**, 118(5), 1221-1222.
- 659 (49) Redmond, R.W.; Gamlin, J.N. A compilation of singlet oxygen yields from biologically  
660 relevant molecules. *Photochem. Photobiol.* **1999**, 70(4), 391-475.
- 661 (50) Torun, L.; Morrison, H. Photooxidation of 2'-deoxyguanosine 5'-monophosphate in  
662 aqueous solution. *Photochem. Photobiol.* **2003**, 77(4), 370-375.
- 663 (51) von Gunten, U. Ozonation of drinking water: Part I. Oxidation kinetics and product  
664 formation. *Water Res.* **2003**, 37(7), 1443-1467.
- 665 (52) Dunge, A.; Chakraborti, A.K.; Singh, S. Mechanistic explanation to the variable  
666 degradation behaviour of stavudine and zidovudine under hydrolytic, oxidative and  
667 photolytic conditions. *J. Pharmaceut. Biomed.* **2004**, 35(4), 965-970.
- 668 (53) Gritsan, N.; Platz M. Photochemistry of azides: The azide/nitrene interface. In  
669 *Organic Azides: Syntheses and Applications*; Bräse, S., Banert, K., Eds.; John Wiley &  
670 Sons; 2010, pp 311-372.
- 671 (54) Iwamoto, T.; Hiraku, Y.; Oikawa, S.; Mizutani, H.; Kojima, M.; Kawanishi, S. Oxidative  
672 DNA damage induced by photodegradation products of 3'-azido-3'-deoxythymidine.  
673 *Archives of Biochemistry and Biophysics.* 2003;416(2):155-163.  
674